Published in final edited form as:

J Orthop Res. 2015 May ; 33(5): 738–746. doi:10.1002/jor.22807.

Alterations in intervertebral disc composition, matrix homeostasis and biomechanical behavior in the UCD-T2DM rat model of type 2 diabetes

Aaron J. Fields[1], **Britta Berg-Johansen**[1], **Lionel N. Metz**[1], **Stephanie Miller**[1], **Brandan La**[1], **Ellen C. Liebenberg**[1], **Dezba G. Coughlin**[1], **James L. Graham**[2,3], **Kimber L. Stanhope**[2,3], **Peter J. Havel**[2,3], and **Jeffrey C. Lotz**[1]

[1]Orthopaedic Bioengineering Laboratory, Department of Orthopaedic Surgery, University of California, San Francisco, CA, United States

[2]Department of Molecular Biosciences, University of California, Davis, CA, United States

[3]Department of Nutrition, University of California, Davis, CA, United States

Abstract

Type 2 diabetes (T2D) adversely affects many tissues, and the greater incidence of discogenic low back pain among diabetic patients suggests that the intervertebral disc is affected too. Using a rat model of polygenic obese T2D, we demonstrate that diabetes compromises several aspects of disc composition, matrix homeostasis and biomechanical behavior. Coccygeal motion segments were harvested from 6-month-old lean Sprague-Dawley rats, obese Sprague-Dawley rats, and diabetic obese UCD-T2DM rats (diabetic for 69 ± 7 days). Findings indicated that diabetes but not obesity reduced disc glycosaminoglycan and water contents, and these degenerative changes correlated with increased vertebral endplate thickness and decreased endplate porosity, and with higher levels of the advanced glycation end-product (AGE) pentosidine. Consistent with their diminished glycosaminoglycan and water contents and their higher AGE levels, discs from diabetic rats were stiffer and exhibited less creep when compressed. At the matrix level, elevated expression of hypoxia-inducible genes and catabolic markers in the discs from diabetic rats coincided with increased oxidative stress and greater interactions between AGEs and one of their receptors (RAGE). Taken together, these findings indicate that endplate sclerosis, increased oxidative stress and AGE/RAGE-mediated interactions could be important factors for explaining the greater incidence of disc pathology in T2D.

Keywords

intervertebral disc degeneration; type 2 diabetes; vertebral endplate; advanced glycation end-products; pentosidine

Address for correspondence: Aaron J. Fields, Ph.D., 513 Parnassus Avenue, S-1161, University of California, San Francisco, CA 94143-0514, United States, Tel: + 1 (415) 476-0960, Fax: + 1 (415) 476-1128, aaron.fields@ucsf.edu.

The authors have no potential conflicts of interest associated with the manuscript.

Introduction

Low back pain (LBP) is among the leading causes of disability and health care expenditures in adults worldwide. The need for improved management of LBP is intensifying with the growing size of the adult population, and is exacerbated by the global epidemic of adult obesity and obesity-related diabetes [1]. Overweight and obese conditions are risk factors for LBP [2, 3]; moreover, diabetes is hypothesized to contribute independently. For example, type 2 diabetes (T2D) appears to increase the frequency and severity of pain [4–7] and is associated with poor treatment outcomes [8, 9]. Since LBP is often related to intervertebral disc degeneration [10], identifying the mechanisms by which T2D affects disc composition and biomechanical behavior is an important step towards improving the management of LBP in diabetes.

Several mechanisms could link T2D with poor disc composition and biomechanical behavior. During the pre-diabetic state, increased insulin levels resulting from insulin resistance can have an anabolic effect on bone metabolism [11]. Any increase in bone formation in the endplate (sclerosis) could negatively impact disc health since the disc is avascular and thus, sclerosis could hinder the transport of nutrients and metabolites across the endplates to and from the disc [12–14]. Hyperglycemia may also be important. Hyperglycemia is associated with ischemic injury that preferentially affects organs with non-redundant end capillary circulation [15, 16]. Accordingly, any injury to the capillary bed adjacent to the endplate could also contribute to disc degeneration by reducing the nutrient supply to the endplate and disc [14].

Besides reducing disc nutrient supply, hyperglycemia could impact the disc directly by increasing the formation of AGEs. AGEs are formed through non-enzymatic glycation of the free amino groups of proteins and lipids by reducing sugars [17]. In normal discs, AGE accumulation has been shown to increase with age [18], trigger catabolic actions within disc cells [19], reduce disc hydration [20], and increase disc tissue stiffness [21]. In diabetes, hyperglycemia accelerates the ordinarily slow rate of endogenous glycation by increasing the availability of sugars that can attach to the amino groups [22]. Ziv *et al*. hypothesized that increased AGE accumulation could underlie the changes in physiochemical properties observed in the discs of diabetic sand rats [23]. More recently, degenerative changes to the disc, including loss of disc height and proteoglycans, were associated with AGE accumulation in type 1 diabetic mice [24]. In humans, AGEs appear to be increased and related to catabolic changes in disc tissues from diabetic patients [25].

Thus, while the links between diabetes and poor disc health are being uncovered [23–25], supporting data remain limited. Here we sought to test the hypothesis that T2D diminishes disc composition, matrix homeostasis and biomechanical behavior, and that these changes are associated with endplate sclerosis, reduced endplate vascular supply, and increased AGE accumulation.

Methods

Study design

A critical component of the study design was its ability to control for the effects of age, disease duration, insulin resistance, obesity, and glycemic control. Since controlling for such effects using a statistical analysis of human tissue obtained during surgery would require a large patient population, we instead relied on a novel rat model of T2D that explicitly controls for these factors and thereby makes it possible to study the effects of diabetes with a much smaller sample size (n = 18 rats total). The University of California at Davis–type 2 diabetes mellitus (UCD-T2DM) rat was developed, characterized and validated to more closely model the pathophysiology of human T2D than other existing rodent models [26]. By crossing two lines of non-diabetic rats — one with adult-onset obesity and insulin resistance, without defects in either leptin production or leptin receptor signaling (obese Sprague-Dawley, OSD) and one with defective pancreatic beta cell islet function and insulin secretion (ZDF-lean) — and selectively breeding the offspring to enrich for diabetes, the subsequent generations demonstrate diabetes in both sexes with adult-onset obesity, insulin-resistance, impaired glucose tolerance, and eventual beta cell decompensation. Advantages of this model over other rodent models of T2D include polygenic rather than monogenic obesity, a later age of onset, intact leptin signaling, preserved fertility, and the development of diabetes in both sexes. Here we compared the UCD-T2DM rats to two non-diabetic control rats: lean Sprague Dawley (LSD) rats and OSD rats. By comparing UCD-T2DM rats to OSD rats — a genetically similar, obese and insulin-resistant control — we sought to disentangle the effects of T2D from the effects of obesity, which is itself an independent risk factor for disc pathology [27].

Animals

Coccygeal (CC) spines were harvested from rats following euthanasia with an overdose of pentobarbital. We focused on coccygeal discs because they are larger and more readily accessible than lumbar discs, which facilitates biochemical and biomechanical analyses. Six-month-old LSD rats (“control”), OSD rats (“obese”), and UCD-T2DM rats (“diabetic”; n = 6 rats/group) were studied. The generation and phenotypes of these rats has been previously described [26]. Rats were maintained and studied in accordance with Institutional Animal Care and Use Committee (IACUC)-approved protocols. Non-fasted blood glucose was monitored every 2 weeks with a glucose meter (LifeScan; Milpitas, CA), and the age of diabetes onset was defined as the age at which hyperglycemia (blood glucose concentration >200 mg/dl on two consecutive measurements) was first detected. Blood was collected for measurement of circulating glucose, insulin, and HbA1c after an overnight fast at the time of killing. Plasma was assayed for glucose and insulin concentrations with an enzymatic colorimetric assay (Fisher Diagnostics; Middleton, VA) and electrochemiluminescence (Meso Scale Discovery; Rockville, MD), respectively. HbA1c was measured with an enzymatic colorimetric assay (Diazyme Laboratories; Poway, CA).

Micro-x-ray computed tomography analysis of endplate microarchitecture (CC4-CC5 segment)

High-resolution X-ray microscopy was performed to quantify bony endplate microarchitecture. Microscopy images of the CC4-CC5 segments were obtained using a Micro-XCT 200 (Xradia Inc.; Pleasanton, CA) with an effective resolution of 5 μm. X-rays were set to a voltage of 50 kVp and a power of 6 W. After image reconstruction, endplate thickness and porosity were evaluated in cylindrical regions of interest (1 mm diameter) adjacent to the nucleus pulposus (Figure 1) [28]. Measurements derived from endplates cranial and caudal to the disc were averaged for each motion segment.

Histologic analysis of endplate vascular supply (CC5-CC6 segment)

Histology was performed to quantify endplate vascular supply in the CC5-CC6 segment. Sections were stained with a solution containing orange G and aniline blue. Images were evaluated for the area of epiphyseal red blood cells (RBCs) using the segmentation function in graphics editing software. The areal fraction of RBCs was defined as the area of RBCs divided by the total area of the epiphyseal marrow space. This analysis was performed for three mid-coronal sections per segment; values from cranial and caudal epiphyses were averaged for each section and segment. Two raters confirmed repeatability for 30 sections ($r = 0.95$, $p < 0.0001$, inter-rater difference in areal fraction of RBCs = 0.06 ± 0.17%).

Biomechanical assessment of creep characteristics (CC6-CC7 segment)

Compressive creep testing was performed to assess the viscoelastic characteristics of the discs [29]. Briefly, the CC6-CC7 segments were cleaned of surrounding tissues, radiographed, potted in casting resin, and mounted into an ElectroForce 3200 load frame (Bose; Eden Prairie, MN). The loading protocol consisted of five cycles of creep for 20 minutes at 0.5 MPa followed by recovery for 40 minutes at 0.1 MPa. Strain-time data from the final creep cycle were fit to a one-dimensional fluid transport model [30]:

$$\varepsilon(t)=\varepsilon_0+\left(\frac{\sigma_0-P_{osm}}{D}-\frac{h_iG}{2kD^2}\right)*\left[1-\exp\left(-\frac{2kDt}{h_i}\right)\right]+\frac{G}{D}t$$

where $\varepsilon(t)$ is the axial strain, ε_0 is the strain at $t = 0$, t is the time, σ_0 is the applied compressive stress, P_{osm} is the initial nucleus swelling pressure, h_i is the initial disc height, k is the permeability of the endplate, D is the strain-dependence of nucleus swelling pressure, and G is the time-dependence of annulus deformation. Least squares curve fitting was used to determine k, D and G for a given set of experimental creep data (MATLAB, The Mathworks Inc.; Natick, MA). Although not a parameter in the model, an initial modulus of the disc was calculated by measuring the slope of the stress-strain curve before the force reached the specified creep load (0.4 MPa/s ramp rate). All tests were performed in PBS at room temperature. Initial disc height and cross-sectional area were estimated from pre-test radiographs.

Biochemical analysis of GAG content (CC6-CC7 segment)

An absorbance assay was used to measure the glycosaminoglycan (GAG) content in the disc. After biomechanical testing, nucleus samples from the CC6-CC7 segment were completely digested in papain solution (20 hours, 60°C). GAG content was determined using a dimethylmethylene blue assay [31]. GAG content was normalized to the dry mass of the nucleus pulposus, which we measured following lyophilization prior to papain digestion. Water content in the nucleus pulposus was calculated from the ratio of the tissue mass measured before and after lyophilization.

Immunoassay of AGE accumulation (CC9-CC10 and CC10-CC11 segments)

ELISA was used to measure the concentration of pentosidine in the disc tissues. Pentosidine is a well-characterized AGE and inter-molecular cross-link that is a sensitive marker of non-enzymatic glycation. Samples of annulus (CC9-CC10) and nucleus (CC10-CC11) were pulverized in a freezer mill and assayed for pentosidine by sandwich ELISA (MyBioSource; San Diego, CA). This ELISA kit has a high sensitivity (0.02 ng/ml) and precision (CV<10%). Pentosidine measurements were normalized to collagen content, which was calculated from the amount of hydroxyproline [32].

PCR assessment of matrix homeostasis (CC8-CC9 segment)

Quantitative PCR was used to characterize matrix homeostasis. Annulus and nucleus samples (CC8-CC9) were homogenized in Trizol (Sigma; St. Louis, MO), and total RNA was collected using phenol chloroform and purified with RNeasy Kits (Qiagen; Valencia, CA). RNA was reverse transcribed using iScript (Bio-Rad; Hercules, CA), and the resulting cDNA was pre-amplified and analyzed via quantitative PCR for the following genes: receptor for AGEs (*Rage*), vascular endothelial growth factor alpha (*Vegfa*), hypoxia-inducible factor 1-alpha (*Hif1a*), insulin-like growth factor-1 (*Igf1*), insulin receptor (*Insr*), glucose transporter 1 (*Slc2a1*), caveolin 1 (*Cav1*), tumor necrosis factor alpha (*Tnfa*), twisted gastrulation protein homolog 1 (*Twsg1*), tissue inhibitor of metalloproteinase 1 (*Timp1*), collagen 2 alpha 1 (*Col2a1*), collagen 1 alpha 1 (*Col1a1*), and aggrecan (*Acan*). The delta-delta Ct method was used to calculate relative expression compared to beta-actin; expression values are reported as fold change over control.

Statistical analysis

ANOVA with Tukey-Kramer post-hoc tests was used to determine the effect of diabetes on the various outcomes. Despite the small sample size (n = 6 rats/group), parametric tests were used because the data were normally distributed ($p > 0.05$, Shapiro-Wilk test). Independent associations between the outcomes were quantified by the Pearson correlation coefficient. All analyses were performed using JMP 11 (SAS Institute; Cary, NC, USA). Significance is defined by $p < 0.05$. Data are given as mean ± SEM.

Results

Blood glucose measurements indicated that the UCD-T2DM rats were diabetic for 69 ± 7 diabetic days. Obese rats and those with diabetes had significantly higher body weights than

age-matched lean controls (Table 1). At sacrifice, diabetic rats also had substantially higher glucose concentrations and HbA1c.

Diabetes diminishes intervertebral disc GAG and water contents

Despite their normal histologic appearance (Figure 2), discs from the diabetic rats demonstrated dramatic biochemical changes that were consistent with the early stages of degeneration. Diabetes but not obesity significantly reduced nucleus GAG content by 51% ($p < 0.005$) and water content by 12% ($p < 0.005$). Radiographic measurements of disc cross-sectional area indicated that discs from obese rats (20.2 ± 0.7 mm^2) and those with diabetes (19.8 ± 1.8 mm^2) were 34% larger than those from lean controls (14.8 ± 1.8 mm^2; $p = 0.02$). The larger disc size can be appreciated in the histologic sections (Figure 2).

Diminished GAG content associates with endplate sclerosis and not reduced vascular supply

Diabetes but not obesity caused endplate sclerosis, with an increase of endplate thickness by 21% ($p < 0.05$) and a close-to-significant decrease of endplate porosity of 41% ($p = 0.08$; Figure 3). When the data were pooled, variations in endplate microarchitecture were significantly correlated with GAG content. GAG content decreased with increasing endplate thickness ($r = -0.56$, $p = 0.02$) and decreasing endplate porosity ($r = 0.47$, $p = 0.05$; Figure 3). Thicker endplates were less porous ($r = -0.61$, $p = 0.008$).

The diminished GAG content also suggested a possible reduction in endplate vascular supply. To investigate this, the quantity of epiphyseal RBCs was estimated from histology. Surprisingly, in both obese non-diabetic and UCD-T2DM diabetic rats, the percentage of RBCs in the epiphysis was increased by 87% and 78% (Figure 4), respectively. This suggests that endplate vascular supply is unlikely to contribute to the diminished GAG content observed in the discs from the diabetic rats.

Diabetes compromises disc biomechanical behavior

Diabetes caused several deleterious changes to biomechanical properties of the disc that had the net effect of reducing creep strain (Figure 5). Diabetes, but not obesity nearly doubled the strain dependence of swelling pressure in the nucleus ($p < 0.05$). Diabetes also decreased the time dependence of annulus deformation compared with the obese non-diabetic group ($p < 0.05$). Analysis of disc stress-strain behavior during the loading ramp indicated that diabetes increased the initial modulus (7.5 ± 0.8 MPa) compared with the obese, non-diabetic rats (3.0 ± 0.4 MPa, $p < 0.005$) and lean control rats (3.8 ± 1.0 MPa, $p < 0.01$). Endplate permeability was similar in all groups ($p = 0.26$).

Diminished biomechanical behavior associated with elevated AGE concentration and lower GAG content

Diabetes, but not obesity significantly increased AGE concentrations in the disc (Figure 6). In the annulus, pentosidine content was elevated by 29% ($p < 0.01$); in the nucleus, by 104% ($p < 0.05$). When the data were pooled from all groups, the variation in nuclear pentosidine content was significantly correlated with the strain dependence of nucleus swelling pressure ($r = 0.49$, $p = 0.04$) and with initial modulus ($r = 0.57$, $p = 0.02$; Figure 6).

Biomechanical behavior also showed independent relationships with water and GAG content. For example, lower GAG content was correlated with increased strain dependence of swelling pressure ($r = -0.58$, $p = 0.01$) and increased initial modulus ($r = -0.64$, $p = 0.004$). The finding that biomechanical outcomes were independently associated with pentosidine and GAG contents reflects potentially important cross-correlations between these results, *i.e.* that increased pentosidine content was highly correlated with lower GAG content ($r = -0.74$, $p = 0.002$).

Diabetes compromises disc matrix homeostasis

Diabetes also shifted disc cell metabolism and matrix homeostasis in a manner that was consistent with increased AGEs and oxidative stress (Figure 7). Diabetes tended to associate with elevated expression of hypoxia-sensitive genes, including *Vegfa* ($p < 0.10$) and *Hif1a* ($p < 0.10$). In the nucleus pulposus, *Rage* expression was up-regulated nine-fold in the diabetic rats (additional rats needed to reach significance), which coincided with their tendency to express lower levels of *Timp1* ($p < 0.10$) and *Col2a1* ($p < 0.05$), and with expressing higher levels of the cytokine *Twsg1* ($p < 0.05$). In the annulus fibrosus, notable findings included elevated expression of the senescence indicator *Cav1* ($p < 0.05$) and of *Twsg1* ($p < 0.05$). Relative to lean controls, diabetic rats also had higher insulin receptor expression in the nucleus (*Insr*, $p < 0.05$) and annulus ($p < 0.10$); *Igf1* expression tended to be higher in the annulus ($p < 0.10$). There was no difference in *Acan* expression, and reliable amplification data were not obtained for *Tnfa*.

Discussion

We report that diabetes significantly undermines disc GAG and water contents, matrix homeostasis, and biomechanical behavior in a rat model of T2D. Most notably, diabetes was associated with a 50% reduction in the GAG content of the disc nucleus and a 12% reduction in disc hydration. For comparison, the magnitude of these differences is comparable to those observed between non-degenerate (Pfirrmann grade 1.9) and moderately degenerate (Pfirrmann grade 3.6) human lumbar discs [33]. Moreover, the diminished GAG and water contents in the diabetic rats coincided with impairments in structural characteristics of the endplate that could influence nutrient transport and with cellular indicators of increased oxidative stress and AGE/RAGE-mediated biological interactions. For example, besides increasing endplate thickness 21% and decreasing endplate porosity 40%, diabetes increased expression of hypoxia-induced genes (*Vegfa*, *Hif1a*) and decreased expression of markers of matrix health (*Timp1, Col2a1*). Diabetes also had negative biomechanical consequences: disc stiffness was increased by 97%, which was correlated with lower GAG content and with elevated levels of the AGE pentosidine. Previous studies suggest a link between diabetes and intervertebral disc degeneration [23], and AGE accumulation is believed to be important [20, 24, 25]. Our results extend those prior findings by demonstrating that endplate sclerosis, increased oxidative stress, and AGE/RAGE-mediated interactions are consequences of T2D that are linked to detrimental changes in the GAG and water content, matrix homeostasis and biomechanical function of the intervertebral disc.

One novel aspect of this study is the use of creep testing for determination of the biomechanical effects of diabetes. Our findings indicate that diabetes significantly reduces disc creep strain and increases disc stiffness, changes that are correlated with increased pentosidine content. This study is the first to demonstrate that diminished biomechanical behavior with diabetes is associated with elevated AGE concentrations. While we are unaware of other studies that assessed disc biomechanical behavior in T2D, our findings are consistent with observations from a study of healthy annulus fibrosus tissue, which showed that glycation increases tissue stiffness in a manner consistent with structural cross-linking [21]. We also found that increased disc stiffness correlated with reduced water content. Disc water content relates to swelling pressure, which is a balance between fixed charge density and tissue stiffness. Importantly, AGEs appear to affect both outcomes. Besides lowering the hydrophilic charge of the GAGs [20], increases in AGEs and one of their receptors *Rage* could elevate the level of reactive oxygen species [34, 35] and induce inflammatory changes that also increase tissue stiffness by promoting matrix catabolism [24, 36, 37]. For example, Illien-Junger *et al.* demonstrated that this AGE-associated catabolic response is implicated in the development of spinal pathology in type 1 diabetic mice [24]. Here we found that *Rage* expression was higher in the nucleus pulposus of the diabetic rats, which coincided with lower *Timp1* and *Col2a1* expression. Taken together, these findings suggest that the dramatic alterations in disc biomechanical behavior with T2D relate to the structural and biological effects of AGEs.

Another novel aspect of this study was the quantification of endplate microarchitecture in diabetic animals. We found T2D caused endplate sclerosis, increasing endplate thickness and decreasing endplate porosity, and that sclerosis correlated with diminished disc GAG content. This study is the first to report that disc degenerative changes occurring with T2D are associated with endplate sclerosis. Although we are unaware of any studies in humans or animals reporting on sclerosis-GAG content relationships in diabetes, similar relationships were reported in discs from non-diabetic humans [12, 28] and rats [13], supporting the generality of our findings. Benneker *et al.* studied discs from donors aged 19–86 years and found that endplate pore density was significantly correlated with adjacent nucleus GAG content [12]. More recently, we reported that donors with thinner and more porous double-layer endplates had higher adjacent GAG/cell when compared with donors that had single-layer endplates [28]. In aging sand rats, Gruber *et al.* reported that increased endplate bone mineral density was correlated with reduced annulus cell viability [13]. Given the consistency of our findings with these prior studies, the collective literature suggests that endplate sclerosis with T2D may be an important factor that contributes to poor disc health.

Disc health also depends on capillaries that supply nutrients to the endplate-disc interface. An unexpected finding was that both obese rats and those with T2D have *increased* RBC density compared with the lean controls. This appears to be inconsistent with the finding that diabetes *decreased* GAG content, yet obesity alone had no appreciable effect. However, Boubriak *et al*. reported that endplate capillary size and density is increased with disc size [14]. In the current study, obese and diabetic rats had 34% greater disc cross-sectional areas, which could explain their greater RBC density. Hence, the diverging GAG contents in those groups is not inconsistent with the increased RBC density; rather, taken together with the

effect of diabetes, but not obesity on endplate microarchitecture, these findings further underscore the possible role of endplate sclerosis in contributing to compromised GAG content and matrix homeostasis in T2D.

Despite its potential importance, the cause of endplate sclerosis in the diabetic rats is unknown. One possible explanation relates to the anabolic effects of insulin on bone metabolism. Insulin stimulates osteoblast activity [38], and accordingly, hyperinsulinemia is associated with increased bone mineral density in humans [39] and rodents [11]. Here, insulin levels were similar in the obese non-diabetic and diabetic rats (1.4 ± 0.3 ng/ml), although the diabetic rats have >2-fold higher insulin levels at diabetes onset (3.4 ± 0.3 ng/ml) [26], which may have contributed to sclerotic endplate changes that persisted following the decline in insulin levels thereafter. Additional factors that could explain the observed endplate sclerosis include the possible remodeling response to AGE-associated bone fragility [40] and/or the osteogenic effects of increased RAGE signaling in chondrocyte-like cells [41, 42].

This study has a number of limitations. Most importantly, we did not study animals with an advanced duration and severity of diabetes, which may limit the generality of the conclusions. However, since diminished GAG content and biomechanical behavior was associated with increased pentosidine content, and because pentosidine content increases with diabetes duration and severity [43], GAG content and biomechanical behavior would both be expected to progressively worsen with a longer duration of diabetes and greater degree of hyperglycemia. This is consistent with findings in bones from hyperglycemic WBN/Kob rats, where AGE-related biomechanical deficits increased with disease duration [44]. A second limitation is that renal failure could contribute independently to the increased AGE accumulation in the diabetic rats. However, while the UCD-T2DM rats show progressive renal dysfunction, it is far from end-stage in the young rats that we studied (data not shown). Thus, any contribution of renal dysfunction to AGE accumulation in our study is likely to be secondary compared to the effects of hyperglycemia and oxidative stress. A third limitation is that we focused on non-enzymatic cross-links rather than on enzymatic cross-links, which have a stabilizing effect on the collagen network and could also be increased by diabetes. Yet data from other rat models of diabetes indicate that changes in enzymatic cross-links are minor compared to the large increases in non-enzymatic cross-links [44, 45], which suggests that measuring enzymatic cross-links would not have altered our conclusions. Finally, analysis of additional rats is needed to confirm some of the gene expression trends. We expect that studying additional rats would not alter the effect size but would instead reduce the reported variances.

In summary, our results show that T2D compromises disc GAG and water contents, matrix homeostasis and biomechanical behavior, and these changes are associated with endplate sclerosis and AGE accumulation. Endplate sclerosis, increased oxidative stress, and AGE/RAGE-mediated interactions in the disc could therefore be important factors contributing to the increased incidence of disc pathology in T2D.

Acknowledgments

Micro-XCT imaging was performed by Sabra Djomehri (Division of Biomaterials and Bioengineering Micro-CT Imaging Facility, UCSF). qPCR was performed by the UCSF Helen Diller Family Comprehensive Cancer Center Genome Analysis Core. This research was funded by grants from the North American Spine Society, the National Institutes of Health (AR063705), Orthopaedic Research and Education Foundation, and the UCSF Diabetes and Endocrinology Research Center. The Micro-CT Imaging Facility at UCSF is funded by the NIH (S10RR026645) and by the Departments of Preventive and Restorative Dental Sciences and Orofacial Sciences at UCSF. The UCD-T2DM rat model was developed and validated, in part with support from NIH grants AT002993, DK-087307, and DK-095980.

Dr. Havel's research program also received support from a Multi-campus Award (#142691) from the UC Office of the President.

References

1. International Diabetes Federation Diabetes Atlas. International Diabetes Federation; 2013.
2. Heuch I, Hagen K, Zwart JA. Body mass index as a risk factor for developing chronic low back pain: a follow-up in the Nord-Trondelag Health Study. Spine. 2013; 38:133–139. [PubMed: 22718225]
3. Shiri R, Karppinen J, Leino-Arjas P, Solovieva S, Viikari-Juntura E. The association between obesity and low back pain: a meta-analysis. Am J Epidemiol. 2010; 171:135–154. [PubMed: 20007994]
4. Licciardone JC, Kearns CM, Hodge LM, Minotti DE. Osteopathic manual treatment in patients with diabetes mellitus and comorbid chronic low back pain: subgroup results from the OSTEOPATHIC Trial. J Am Osteopath Assoc. 2013; 113:468–478. [PubMed: 23739758]
5. Mantyselka P, Miettola J, Niskanen L, Kumpusalo E. Chronic pain, impaired glucose tolerance and diabetes: a community-based study. Pain. 2008; 137:34–40. [PubMed: 17869422]
6. Lotan R, Oron A, Anekstein Y, Shalmon E, Mirovsky Y. Lumbar stenosis and systemic diseases: is there any relevance? J Spinal Disord Tech. 2008; 21:247–251. [PubMed: 18525484]
7. Sakellaridis N. The influence of diabetes mellitus on lumbar intervertebral disk herniation. Surg Neurol. 2006; 66:152–154. [PubMed: 16876608]
8. Takahashi S, Suzuki A, Toyoda H, et al. Characteristics of diabetes associated with poor improvements in clinical outcomes after lumbar spine surgery. Spine. 2013; 38:516–522. [PubMed: 22976346]
9. Freedman MK, Hilibrand AS, Blood EA, et al. The impact of diabetes on the outcomes of surgical and nonsurgical treatment of patients in the spine patient outcomes research trial. Spine. 2011; 36:290–307. [PubMed: 21270715]
10. Luoma K, Riihimaki H, Luukkonen R, Raininko R, Viikari-Juntura E, Lamminen A. Low back pain in relation to lumbar disc degeneration. Spine. 2000; 25:487–492. [PubMed: 10707396]
11. Prisby RD, Swift JM, Bloomfield SA, Hogan HA, Delp MD. Altered bone mass, geometry and mechanical properties during the development and progression of type 2 diabetes in the Zucker diabetic fatty rat. J Endocrinol. 2008; 199:379–388. [PubMed: 18755885]
12. Benneker LM, Heini PF, Alini M, Anderson SE, Ito K. 2004 Young Investigator Award Winner: vertebral endplate marrow contact channel occlusions and intervertebral disc degeneration. Spine. 2005; 30:167–173. [PubMed: 15644751]
13. Gruber HE, Gordon B, Norton HJ, et al. Analysis of cell death and vertebral end plate bone mineral density in the annulus of the aging sand rat. Spine J. 2008; 8:475–481. [PubMed: 18455112]
14. Boubriak OA, Watson N, Sivan SS, Stubbens N, Urban JP. Factors regulating viable cell density in the intervertebral disc: blood supply in relation to disc height. J Anat. 2013; 222:341–348. [PubMed: 23311982]
15. Hammes HP, Alt A, Niwa T, et al. Differential accumulation of advanced glycation end products in the course of diabetic retinopathy. Diabetologia. 1999; 42:728–736. [PubMed: 10382593]

16. Teillet L, Verbeke P, Gouraud S, et al. Food restriction prevents advanced glycation end product accumulation and retards kidney aging in lean rats. J Am Soc Nephrol. 2000; 11:1488–1497. [PubMed: 10906162]
17. Peppa M, Uribarri J, Vlassara H. Glucose, advanced glycation end products, and diabetes complications: what is new and what works. Clin Diabetes. 2003; 21:186–187.
18. Sivan SS, Tsitron E, Wachtel E, et al. Age-related accumulation of pentosidine in aggrecan and collagen from normal and degenerate human intervertebral discs. Biochem J. 2006; 399:29–35. [PubMed: 16787390]
19. Yokosuka K, Park JS, Jimbo K, et al. Advanced glycation end-products downregulating intervertebral disc cell production of proteoglycans in vitro. J Neurosurg Spine. 2006; 5:324–329. [PubMed: 17048769]
20. Jazini E, Sharan AD, Morse LJ, et al. Alterations in T2 relaxation magnetic resonance imaging of the ovine intervertebral disc due to nonenzymatic glycation. Spine. 2012; 37:E209–215. [PubMed: 21857410]
21. Wagner DR, Reiser KM, Lotz JC. Glycation increases human annulus fibrosus stiffness in both experimental measurements and theoretical predictions. J Biomech. 2006; 39:1021–1029. [PubMed: 15878594]
22. Ahmed N. Advanced glycation endproducts--role in pathology of diabetic complications. Diabetes Res Clin Pract. 2005; 67:3–21. [PubMed: 15620429]
23. Ziv I, Moskowitz RW, Kraise I, Adler JH, Maroudas A. Physicochemical properties of the aging and diabetic sand rat intervertebral disc. J Orthop Res. 1992; 10:205–210. [PubMed: 1740738]
24. Illien-Junger S, Grosjean F, Laudier DM, Vlassara H, Striker GE, Iatridis JC. Combined anti-inflammatory and anti-AGE drug treatments have a protective effect on intervertebral discs in mice with diabetes. PLoS One. 2013; 8:e64302. [PubMed: 23691192]
25. Tsai TT, Ho NY, Lin YT, et al. Advanced glycation end products in degenerative nucleus pulposus with diabetes. J Orthop Res. 2014; 32:238–244. [PubMed: 24151186]
26. Cummings BP, Digitale EK, Stanhope KL, et al. Development and characterization of a novel rat model of type 2 diabetes mellitus: the UC Davis type 2 diabetes mellitus UCD-T2DM rat. Am J Physiol Regul Integr Comp Physiol. 2008; 295:R1782–1793. [PubMed: 18832086]
27. Samartzis D, Karppinen J, Chan D, Luk KD, Cheung KM. The association of lumbar intervertebral disc degeneration on magnetic resonance imaging with body mass index in overweight and obese adults: a population-based study. Arthritis Rheum. 2012; 64:1488–1496. [PubMed: 22287295]
28. Fields AJ, Sahli Costabal F, Rodriguez AG, Lotz JC. Seeing double: A comparison of microstructure, biomechanical function and adjacent disc health between double- and single-layer vertebral endplates. Spine. 2012; 37:E1310–1317. [PubMed: 22781006]
29. Palmer EI, Lotz JC. The compressive creep properties of normal and degenerated murine intervertebral discs. J Orthop Res. 2004; 22:164–169. [PubMed: 14656676]
30. Cassidy JJ, Silverstein MS, Hiltner A, Baer E. A water transport model for the creep response of the intervertebral disc. J Mater Sci Mater Med. 1990; 1:81–89.
31. Farndale RW, Buttle DJ, Barrett AJ. Improved quantitation and discrimination of sulphated glycosaminoglycans by use of dimethylmethylene blue. Biochim Biophys Acta. 1986; 883:173–177. [PubMed: 3091074]
32. Woessner JF Jr. The determination of hydroxyproline in tissue and protein samples containing small proportions of this imino acid. Arch Biochem Biophys. 1961; 93:440–447. [PubMed: 13786180]
33. Nguyen AM, Johannessen W, Yoder JH, et al. Noninvasive quantification of human nucleus pulposus pressure with use of T1rho-weighted magnetic resonance imaging. J Bone Joint Surg Am. 2008; 90:796–802. [PubMed: 18381318]
34. Coughlan MT, Thorburn DR, Penfold SA, et al. RAGE-induced cytosolic ROS promote mitochondrial superoxide generation in diabetes. J Am Soc Nephrol. 2009; 20:742–752. [PubMed: 19158353]
35. Reiser KM. Nonenzymatic glycation of collagen in aging and diabetes. Proc Soc Exp Biol Med. 1998; 218:23–37. [PubMed: 9572149]

36. Nasto LA, Robinson AR, Ngo K, et al. Mitochondrial-derived reactive oxygen species (ROS) play a causal role in aging-related intervertebral disc degeneration. J Orthop Res. 2013; 31:1150–1157. [PubMed: 23389888]
37. Stern DM, Yan SD, Yan SF, Schmidt AM. Receptor for advanced glycation endproducts (RAGE) and the complications of diabetes. Ageing Res Rev. 2002; 1:1–15. [PubMed: 12039445]
38. Raisz LG, Kream BE. Regulation of bone formation. N Engl J Med. 1983; 309:29–35. [PubMed: 6343872]
39. Rishaug U, Birkeland KI, Falch JA, Vaaler S. Bone mass in non-insulin-dependent diabetes mellitus. Scand J Clin Lab Invest. 1995; 55:257–262. [PubMed: 7638560]
40. Tang SY, Zeenath U, Vashishth D. Effects of non-enzymatic glycation on cancellous bone fragility. Bone. 2007; 40:1144–1151. [PubMed: 17257914]
41. Loeser RF, Yammani RR, Carlson CS, et al. Articular chondrocytes express the receptor for advanced glycation end products: Potential role in osteoarthritis. Arthritis Rheum. 2005; 52:2376–2385. [PubMed: 16052547]
42. Ott C, Jacobs K, Haucke E, Navarrete Santos A, Grune T, Simm A. Role of advanced glycation end products in cellular signaling. Redox Biol. 2014; 2:411–429. [PubMed: 24624331]
43. Sugiyama S, Miyata T, Ueda Y, et al. Plasma levels of pentosidine in diabetic patients: an advanced glycation end product. J Am Soc Nephrol. 1998; 9:1681–1688. [PubMed: 9727377]
44. Saito M, Fujii K, Mori Y, Marumo K. Role of collagen enzymatic and glycation induced cross-links as a determinant of bone quality in spontaneously diabetic WBN/Kob rats. Osteoporos Int. 2006; 17:1514–1523. [PubMed: 16770520]
45. Pokharna HK, Boja B, Monnier VM, Moskowitz RW. Effect of age on pyridinoline and pentosidine matrix cross-links in the desert sand rat intervertebral disc. Glycosyl Dis. 1994; 1:185–190.

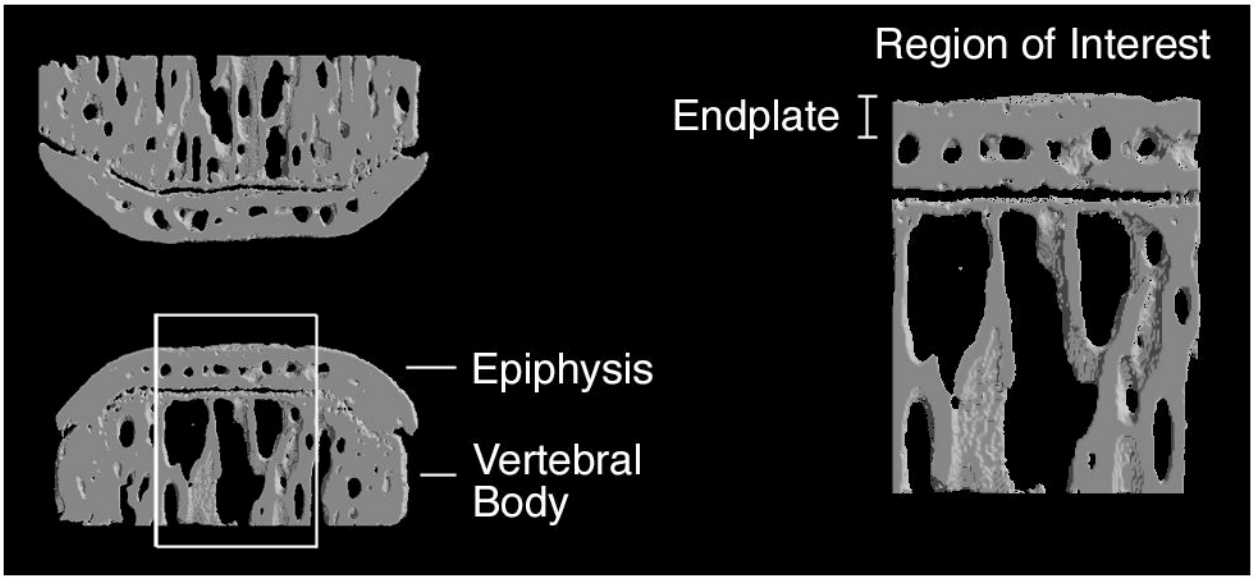

Figure 1.
Reconstructed micro-tomography cross-section (50 μm-thick) illustrating the location of the region of interest for measurement of endplate thickness and porosity.

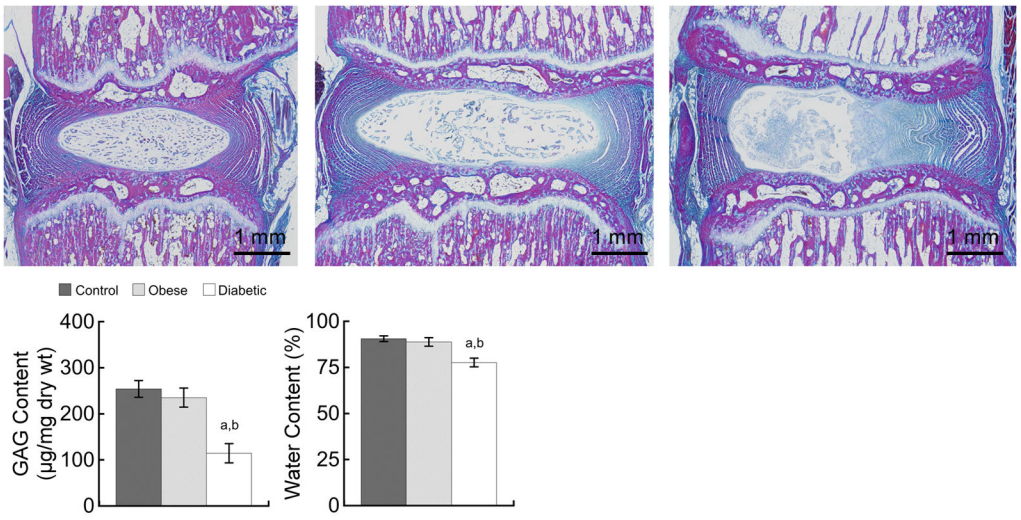

Figure 2.

Top- Mid-coronal histology sections from control (left), obese (center), and diabetic (right). Heidenhain connective tissue stain. **Bottom-** Effect of diabetes and obesity on GAG content (left) and water content (right) in the nucleus pulposus. Mean ± SEM for $n = 6$ rats/group; [a] $p < 0.005$ vs. control, [b] $p < 0.005$ vs. obese.

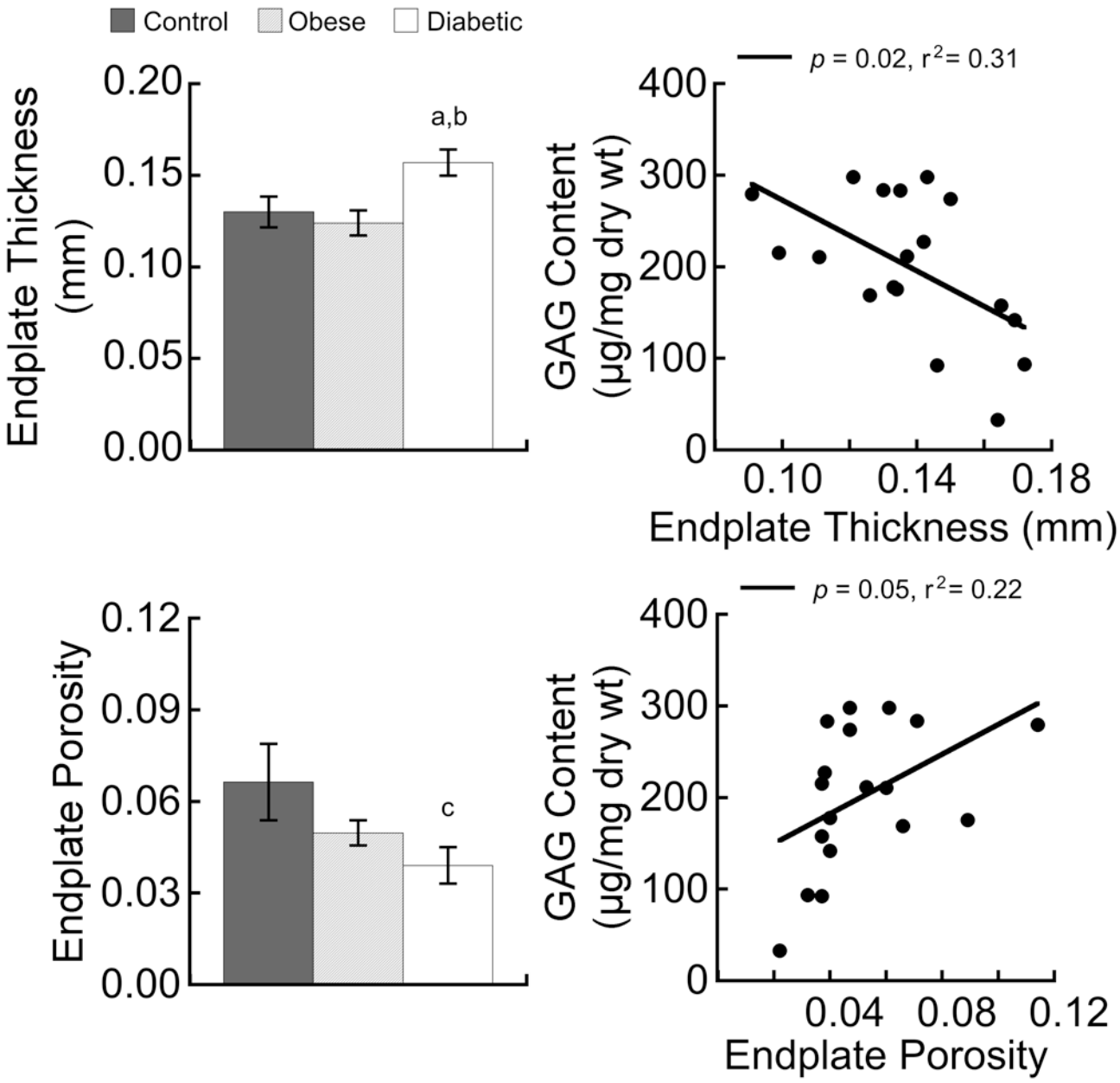

Figure 3.

Top- Diabetes significantly increased endplate thickness (left) and greater thickness correlated with reduced GAG content (right). **Bottom-** Diabetes tended to decrease endplate porosity (left), and reduced porosity correlated with reduced GAG content (right). Mean ± SEM for $n = 6$ rats/group; [a] $p < 0.05$ vs. control, [b] $p < 0.05$ vs. obese, [c] $p < 0.10$ vs. control. Scatter plot data are pooled from all groups.

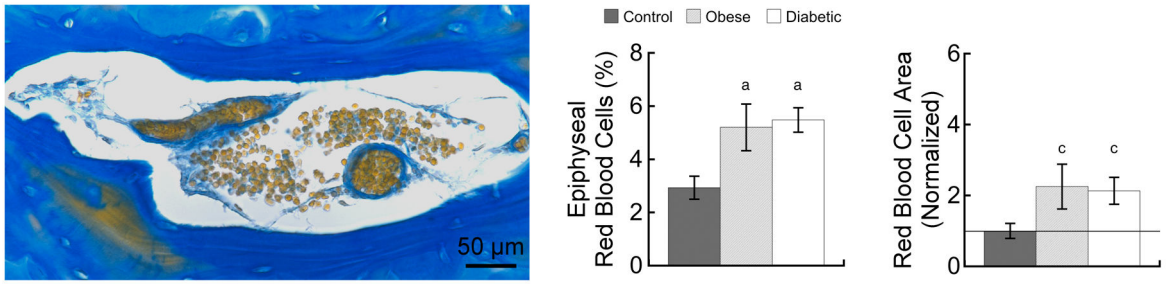

Figure 4.

Photomicrograph showing the epiphyseal bone marrow cavity from a diabetic rat (left). Custom stain: RBCs are stained orange; vessel walls and bone matrix are stained blue. Diabetes and obesity significantly increased the percentage of the epiphyseal marrow space occupied by RBCs (center). In absolute terms, diabetes and obesity tended to double the area of RBCs (right; values normalized to the 'control' group). Mean ± SEM for n = 4–7 rats/group; [a] $p < 0.05$ vs. control; [c] $p < 0.10$ vs. control.

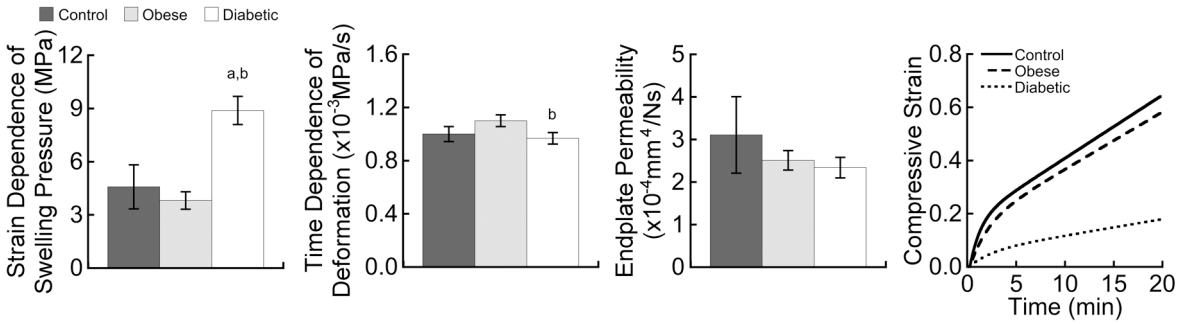

Figure 5.

Effect of diabetes and obesity on creep properties. Creep behavior (right) showed that discs from the diabetic rats compressed less under the constant applied stress, indicating they were stiffer. Mean ± SEM for n = 5–6 rats/group; [a] $p < 0.05$ vs. control, [b] $p < 0.05$ vs. obese.

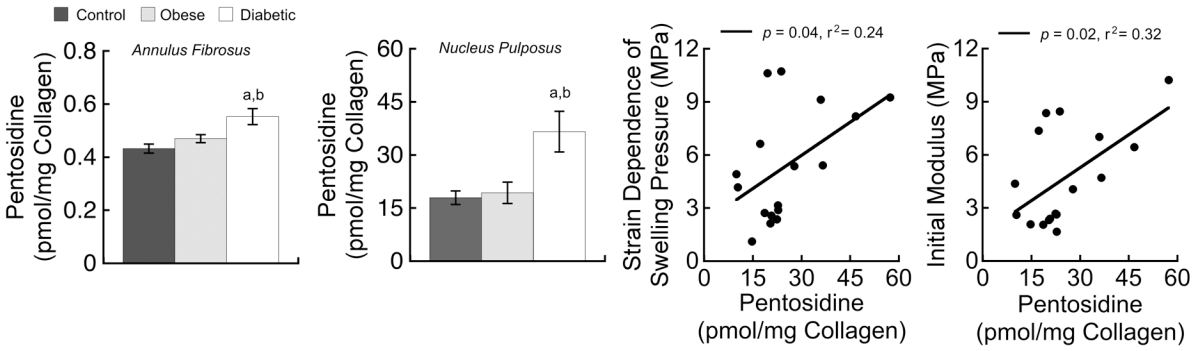

Figure 6.

Diabetes but not obesity significantly increased pentosidine content in the annulus fibrosus and nucleus pulposus, and greater nucleus pentosidine content correlated with greater strain dependence of swelling pressure and initial modulus. Mean ± SEM for $n = 6$ rats/group; [a] $p < 0.01$ vs. control, [b] $p < 0.05$ vs. obese. Scatter plot data are pooled from all groups.

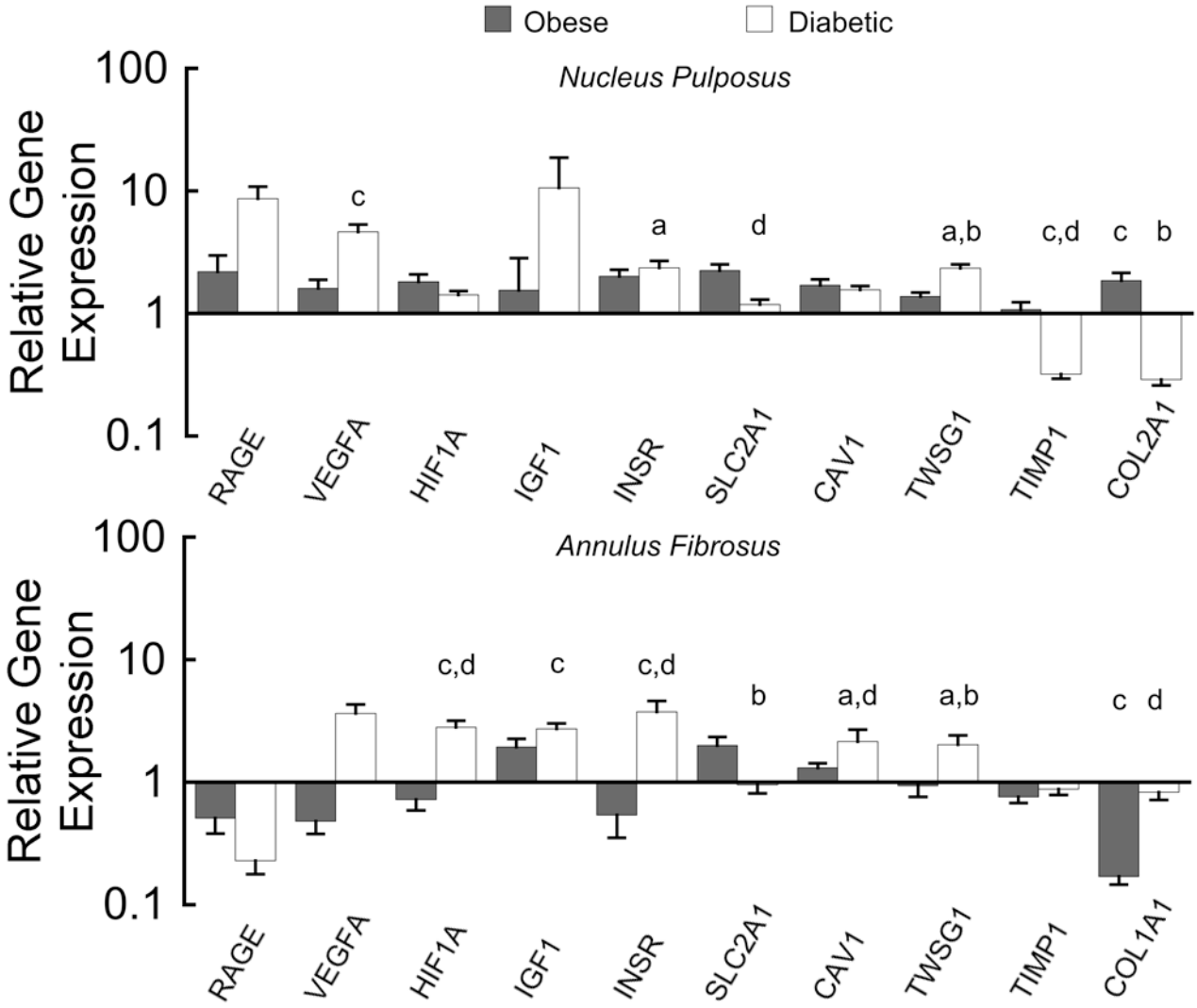

Figure 7.

Effect of diabetes and obesity on disc gene expression (fold changes relative to control rats). Mean ± SEM for n = 5–6 rats/group; letters indicate significant and trending differences with >2-fold change; [a] $p < 0.05$ vs. control, [b] $p < 0.05$ vs. obese, [c] $p < 0.10$ vs. control, [d] $p < 0.10$ vs. obese.

Table 1

Body weight, glucose, insulin, and HbA1c data for control, obese, and diabetic rats. All rats aged 6 mo.

	Control – Lean Sprague Dawley (*n* = 5 rats)	**Obese – Obese Sprague Dawley (*n* = 6 rats)**	**Diabetic – UCD-T2DM (*n* = 6 rats)**
Duration of diabetes (days)	NA	NA	69 ± 7
Body weight (g)	426.0 ± 12.1	693.7 ± 29.0[a]	563.5 ± 18.9[c,d]
Non-fasting glucose (mg/dl)	112.2 ± 3.4	112.2 ± 4.7	546.2 ± 18.5[a,b]
Fasting glucose (mg/dl)	91.8 ± 3.2	98.7 ± 2.8	246.4 ± 52.6[c,d]
Fasting insulin (ng/ml)	0.6 ± 0.07	1.4 ± 0.2[e]	1.4 ± 0.3[e]
HbA1c (%)	4.5 ± 0.09	4.3 ± 0.06	11.8 ± 1.28[a,b]
HbA1c (mmol/mol)	26.0 ± 1.0	23.8 ± 0.7	105 ± 14.0

All data given as mean ± SEM.

NA – Not applicable

[a] $p < 0.0001$ *vs.* control.

[b] $p < 0.0001$ *vs.* obese.

[c] $p < 0.05$ *vs.* control.

[d] $p < 0.05$ *vs.* obese.

[e] $p < 0.10$ *vs.* control.